Distributionally Robust Data Join for Image Classification

Anderson Lee
Department of Computer Science
University of Washington
Seattle, WA 98195
lee0618@cs.washington.edu

Rachel Hong
Department of Computer Science
University of Washington
Seattle, WA 98195
hongrach@cs.washington.edu

Abstract

Distribution shift in image classification task has been a significant problem that compromises model's performance after deployment. Distributionally Robust Optimization (DRO) has been well-studied to train robust models for distribution shift by optimizing the worst case loss of a set of candidate distributions around an empirical distribution. In this paper, we study the adaptation of the method proposed in [1] to incorporate unlabeled dataset with auxiliary features to provide the set of candidate distributions to optimize over, in the context of image classification tasks. We further propose an alternative adversarial training approach which inherits the motivation and is more tractable for deep neural network. In experiments on CIFAR-100 and CIFAR-100C [2], we are able to observe some robustness when evaluated on severely corrupted images.

1 Introduction

Distribution shift is more than common in image classification task such as background changes in the wild for different camera traps, tumor identification data from different hospitals, and autonomous driving decision-making when real-world scene changes. [3, 4] While deep neural network and vision transformer become more prevalent in high-stake classification tasks such as medical image scan and autonomous driving, ensuring the robustness of model on out-of-distribution inference is essential and requires different sets of training approaches than classical empirical risk minimization. Two main approaches to improve model's robustness are Distributionally Robust Optimization and Adversarial Training.

Distributionally Robust Optimization (DRO) has been a well-studied approach to train a distributionally robust model by optimizing the worst case distribution loss around the empirical distribution. [5] The set of distributions to be considered is often called *ambiguity set*. A common phenomenon when solving distributionally robust optimization problem to train a predictor is that the predictor becomes overly-pessimistic and is not able to confidently predict any outcome. This phenomenon usually arises from having a too large ambiguity set that encompasses non-tractable worst case distribution. The methods to determine the ambiguity set are therefore important in order to include the ideal wild distribution in the ambiguity set while not including to many unlikely distributions to optimize the model over.

There have been multiple studies on how to define a good ambiguity set in both the definition of distance metrics that render the ambiguity set to be centered around the empirical distribution within some radius such as Prohorov metric [6] and Wasserstein metric [7]. Another set of methods to formulate ambiguity set is to utilize the moment of probability distributions such as *Chebyshev ambiguity set*. [5]

Preprint. Under review.

In addition to choosing the definition of ambiguity set, another level beyond is to further articulate the ambiguity set for a certain classification task. [8] proposes a modified loss function to optimize extending from traditional DRO objective in favor of the emphasis on group information shift during inference time. [1] takes advantages of unlabeled dataset with auxiliary features to define the ambiguity set with Wasserstein metric. Similarly, [9] incorporates unlabeled data to formulate the DRO objective to derive a tractable ambiguity set.

Adversarial Training (AT) perturbs training data as a way to simulate distribution shift or even worse and unrealistic case. While AT perturbs each sample in different ways, DRO focuses on the entire distribution shift. AT can be viewed as shifting the empirical distribution to some point around itself depending on the actual implementation. In other words, in the perspective of ambiguity set, it's a set with a singular point. [10] shows that a lower bound of AT loss on point-wise perturbation by the worst case distribution loss. In the context of image classification, [11] incorporates unlabeled images to perform AT and shows improvement in both accuracy and robustness.

While unlabeled data is commonly believed to be much more accessible than labeled data, there have been only a few works on utilizing unlabeled data to improve both robustness and performance of the model. Beyond unlabeled data with the same set of features, auxiliary features in unlabeled data are also common such as in the context of medical data from different hospitals or wildlife images from different monitoring institutions. Taking advantage of the auxiliary features or even multimodal features to train a joint distribution predictor or even one with performative marginal prediction with a subset of features can be potential as a way to refine the ambiguity set.

In this work, we follow up the empirical work in the context of image classification task to take advantage of theoretical guarantees on the robustness in [1]. Besides, we also present an AT approach that intuitively simulates the motivation with more randomness and less theoretical backbone but with easier implementation and training stability.

2 Problem Setup

2.1 Distributionally Robust Data Join (DRDJ)

In [1], two datasets S_A and S_P are given where S_A is an unlabeled dataset with shared features x and auxiliary features a and S_P is a labeled dataset with shared features x and labels y. The respective empirical distributions of S_A, S_P are denoted as $\tilde{\mathcal{P}}_{S_A}$ and $\tilde{\mathcal{P}}_{S_P}$. The ambiguity set defined is

$$W(S_A, S_P, r_A, r_P) = \{\mathcal{Q} \in \mathbb{P}_{(\mathcal{X},\mathcal{A},\mathcal{Y})} : \mathcal{D}_{d_A}(\mathcal{Q}_{\mathcal{X},\mathcal{A}}, \tilde{\mathcal{P}}_{S_A}) \leq r_A, \mathcal{D}_{d_P}(\mathcal{Q}_{\mathcal{X},\mathcal{Y}}, \tilde{\mathcal{P}}_{S_P}) \leq r_P\}$$

where $\mathcal{D}_{d_A}$ is Wasserstein distance between marginalized $\mathcal{Q}_{\mathcal{X},\mathcal{A}}$ and the empirical unlabeled distribution $\tilde{\mathcal{P}}_{S_A}$, and $\mathcal{D}_{d_P}$ represents the counterparts in empirical labeled distribution. r_A, r_P represent the radius of the Wasserstein distance ball around the empirical distribution $\tilde{\mathcal{P}}_{S_A}$ and $\tilde{\mathcal{P}}_{S_P}$ respectively. Intuitively, this ambiguity set represents the intersection between the Wesserstein ball around two empirical distributions with constant parameter radius r_A, r_P. The objective of DRO following this ambiguity set is

$$\min_{\theta \in \Theta} \sup_{\mathcal{Q} \in W(S_A, S_P, r_A, r_P)} \mathbb{E}_{(x,a,y)\in\mathcal{Q}}[\ell(\theta, (x, a, y))]$$

where $\ell : \Theta \times (\mathcal{X} \times \mathcal{A} \times \mathcal{Y}) \to \mathbb{R}$ is the convex loss function, and θ is the model parameters.

2.2 Original Objectives

[1] derives two objectives to optimize over simultaneously through a series of duality and problem reduction in the context of logistic regression.

$$\begin{aligned}
&\Omega^A(\alpha_A, \alpha_P, \theta) \\
&= \min_{\alpha_A \alpha_P \theta_1 \theta_2} (\alpha_A r_A + \alpha_P r_P) + \frac{1}{n_A n_P} \sum_{(i,j) \in M} (f(y_j^P \langle \theta, (x_j^P, a_i^A) \rangle) \\
&\quad + \max(y_j^P \langle \theta, (x_j^P, a_i^A) \rangle - \alpha_P \kappa_P, 0) - \alpha_A ||x_i^A - x_j^P||) \\
&\Omega^P(\alpha_A, \alpha_P, \theta) \\
&= \min_{\alpha_A \alpha_P \theta_1 \theta_2} (\alpha_A r_A + \alpha_P r_P) + \frac{1}{n_A n_P} \sum_{(i,j) \in M} (f(y_j^P \langle \theta, (x_i^A, a_i^A) \rangle) \\
&\quad + \max(y_j^P \langle \theta, (x_j^P, a_i^A) \rangle - \alpha_P \kappa_P, 0) - \alpha_P ||x_i^A - x_j^P||)
\end{aligned}$$

constrained by

$$\begin{aligned}
C^A &= \{(\alpha_A, \alpha_P, \theta) : ||\theta_1||_* \leq \alpha_A + \alpha_P, ||\theta_2|| \leq \kappa_A \alpha_A, \alpha_A < \alpha_P\} \\
C^P &= \{(\alpha_A, \alpha_P, \theta) : ||\theta_1||_* \leq \alpha_A + \alpha_P, ||\theta_2|| \leq \kappa_A \alpha_A, \alpha_A > \alpha_P\}
\end{aligned}$$

for each objective respectively.

Notations. x_i^A represents the ith sample from S_A, and x_j^P represents the jth sample from S_P. M represents *matching pairs*. (i, j) exists in M if and only if the shared features x_i^A from S_A is in the k-nearest neighbor of x_j^P from S_P or the other way around. α_A and α_P are trainable parameters resulting from duality of the original optimization problem. κ_A and κ_P are hyperparameters from duality of the original optimization problem as well. θ_1 denotes the linear weights for shared features x and θ_2 denotes the linear weights for auxiliary features a. θ is the concatenation of θ_1 and θ_2. The resulting θ will come from the minimum of these two objectives after optimizing. $f(t)$ represents logistic loss $\log(1 + \exp(t))$.

3 Multi-class Vanilla DRDJ Objective Optimization

3.1 Image Classification Adaptation

Loss function. We first replace the original logistic loss f in the objective with cross entropy loss to support multiple classes

Norm difference. The norm term $||x_i^A - x_j^P||$ aims to present the similarity between two shared features in a matching pair. However, since image data has higher dimensionality and complexity, direct comparison will not result in desirable property. We replace the norm term by the embeddings of images before final linear classifier layer $g(\theta, x_j^P, a_i^A)$. We use $g(\theta, x_j^P, a_i^A)$ to represent the trained model.

Inner product. The inner product $\langle \theta, (x_j^P, a_i^A) \rangle$ in Ω^A comes from vanilla logistic regression. In multi-class image classification task, we use predicted logits instead. From the previous notation, the predicted logits are denoted as Linear$(g(\theta, x_j^P, a_i^A))$ where the linear layer outputs number of classes according to the classification task.

3.2 kNN Matching Pairs

In the proposed algorithm from [1], kNN is used for each sample in both S_A and S_P to generate the matching pairs M as described above. However, for high dimensional data like images, it is significantly more difficult and less meaningful to naively do a similarity search on raw images using kNN algorithms.

We first adopted SOTA masked autoencoder [12] to find a lower dimensional representation of each image as their embeddings. Then, we perform similarity search on those embeddings as the source for generating matching pairs images. However, in our first batch of experiments, we were not able to

generate good matching pairs based on qualitative analysis. For the time-constraint of this project, we simplify the matching pairs generation by using their ground truth labels even for the allegedly unlabeled dataset. The exact procedure is further specified in Section 5.1.

3.3 Constraint Set

In the original objective, the constraints C^A and C^P for Ω^A and Ω^P respectively are enforced by Projected Gradient Descent for optimization in the experiments in the original paper [1]. However, implementing Projected Gradient Descent on GPU and PyTorch framework is quite difficult and doesn't have off-the-shelf supports from other packages. Therefore, we use penalty term to penalize solutions that violate the constraints sets. Specifically, there are three different penalty terms with different hyperparameter $\lambda_1, \lambda_2, \lambda_3$.

In addition, since we are no longer in the realm of classical logistic regression, we cannot provide upper-bound on all parameters. Therefore, to simplify the problem, we only penalize on the weight parameters of the final classifier layer.

$$\text{Penalty}^A = \lambda_1 \cdot (||\theta_1||_* - (\alpha_A + \alpha_P)) + \lambda_2 \cdot (||\theta_2|| - \kappa_A \alpha_A) + \lambda_3 \cdot (\alpha_A - \alpha_P)$$
$$\text{Penalty}^P = \lambda_1 \cdot (||\theta_1||_* - (\alpha_A + \alpha_P)) + \lambda_2 \cdot (||\theta_2|| - \kappa_A \alpha_A) + \lambda_3 \cdot (\alpha_P - \alpha_A)$$

3.4 Vanilla DRDJ Objective

With the above adaptations and simplifications, the objective to optimize over becomes

$$\begin{aligned}
&\Omega^A(\alpha_A, \alpha_P, \theta) \\
&= \min_{\alpha_A \alpha_P \theta_1 \theta_2} (\alpha_A r_A + \alpha_P r_P) + \frac{1}{n_A n_P} \sum_{(i,j) \in M} (\text{CrossEntropyLoss}(\text{Linear}(g(\theta, x_j^P, a_i^A)), y_j^P) \\
&\quad + \max(\text{Linear}(g(\theta, x_j^P, a_i^A))_{y_j} - \alpha_P \kappa_P, 0) - \alpha_A ||g(\theta, x_i^A) - g(\theta, x_j^P)||) \\
&\Omega^P(\alpha_A, \alpha_P, \theta) \\
&= \min_{\alpha_A \alpha_P \theta_1 \theta_2} (\alpha_A r_A + \alpha_P r_P) + \frac{1}{n_A n_P} \sum_{(i,j) \in M} (\text{CrossEntropyLoss}(\text{Linear}(g(\theta, x_i^A, a_i^A)), y_j^P) \\
&\quad + \max(\text{Linear}(g(\theta, x_j^P, a_i^A))_{y_j} - \alpha_P \kappa_P, 0) - \alpha_P ||g(\theta, x_i^A) - g(\theta, x_j^P)||)
\end{aligned}$$

4 Distributionally Robust Adversarial Attack

4.1 Intuition

The motivation of data join for distributionally robust optimization is to take advantage of an anchor distribution (the unlabeled dataset) and to believe that training the model by optimizing the worst case loss in the set of distributions within the intersection of the Wasserstein balls around two empirical distributions will lead to a more robust model. Instead of optimizing the objective that is intrinsically difficult because of the theoretical constraints, it might be more desirable and easier to implement perturbation as adversarial attack that simulates the motivation.

Figure 1 shows the intuition of optimizing over the intersection ambiguity set in original DRDJ. We can simulate the set of distributions by leveraging original samples from two empirical distributions and perturbed samples. [10] uses point-wise adversarial training as an alternative of traditional DRO objective where ambiguity set is defined as a Wasserstein ball around a single empirical distribution. In our case, since we are interested in an intersected set of distributions, a doubly constrained adversarial perturbation is still less feasible. Instead, we perform separate perturbations on the two samples we have, x_i^A, x_j^P in a matching pair defined the same way as vanilla DRDJ.

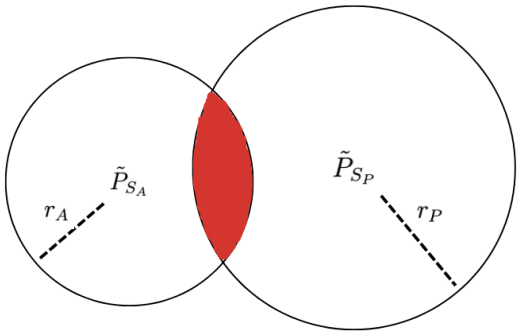

Figure 1: Wasserstein Ball Ambiguity Set

4.2 Perturbation

We define $\tilde{x}_i^A$ as the perturbed sample of x_i^A and $\tilde{x}_j^P$ as the perturbed sample of x_j^P. They are formally defined as

$$\tilde{x}_i^A = \arg \max_{x \in \mathcal{B}(x_i^A, r_A)} ||\text{Linear}(g(\theta, x, a_i^A)) - \text{Linear}(g(\theta, x_j^P, a_i^A))||_2$$
$$\tilde{x}_j^P = \arg \max_{x \in \mathcal{B}(x_j^P, r_P)} ||\text{Linear}(g(\theta, x_i^A, a_i^A)) - \text{Linear}(g(\theta, x, a_i^A))||_2$$

where x_i^A, x_j^P inherit the notations from above in a matching pair, $\mathcal{B}(x_i^A, r_A)$ denotes a L2-norm ball with radius r_A around x_i^A, and $\mathcal{B}(x_j^P, r_P)$ denotes a L2-norm ball with radius r_P around x_j^P.

These two perturbed samples can be viewed as the samples close to the original sample (x_i^A or x_j^P) within some radius in a L2-norm ball that make their predicted logits the **most different** from the *anchor sample* which is the other original sample that is not being perturbed (e.g. x_i^A is the anchor if perturbing x_j^P). The perturbed samples are not at all guaranteed to be located in the intersected set because there exists no constraint on the radius with the other ball. In fact, it's more likely that they are located on the opposite direction of the other anchor sample because the optimization problem maximizes the difference of predicted logits between them. We believe that optimizing over both of them with some hyperparameter weights at the same time will be sufficient to perform well on the intersected set of interest because a well-trained predictor should balance the performance well on samples extremely far from $\tilde{P}_{S_A}$ and close to $\tilde{P}_{S_P}$ or the other way around.

4.3 Loss Function

With perturbed samples, we can weigh the Cross-entropy loss of original samples and adversarial samples in training time to emphasize the focus on perturbed samples or empirical distribution. The motivation to weigh in the empirical loss instead of only the perturbed sample loss is to guide the model to learn the classification task in earlier training time as the perturbation depends on the model's ability to differentiate predicted logits from different types of images. In other words, the perturbation task requires the model's predictive power in order to be significantly meaningful. Thus, the loss function can be formally defined as

$$L_{\text{adversarial}} = w_1 \cdot \ell(\theta, (x_j^p, y_j^p)) + w_2 \cdot \ell(\theta, (\tilde{x}_j^p, y_j^p)) + w_3 \cdot \ell(\theta, (x_i^a, y_j^p)) + w_4 \cdot \ell(\theta, (\tilde{x}_i^a, y_j^p))$$

4.4 Training Schedule

5 Experiments

5.1 Setup

Due to time constraints, the main experiments were done in CIFAR-100 image dataset. Instead of trying to work with two datasets with one labeled and the other unlabeled and equipped with

Algorithm 1 Adversarial DRDJ Train One Epoch

for $X_i^A, A_i^A, X_j^P, Y_j^P$ in batch **do**
    $\tilde{X}_i^A, \tilde{X}_j^P \leftarrow$ Solve argmax problem
    Calculate loss function $L_{\text{adversarial}}$
    Backward Propagation as usual
end for

auxiliary features, we simplify the problem to focus on **splitting CIFAR-100 to two subsets** and **limit ourselves to no auxiliary features for images** for time being.

CIFAR-100 contains 60,000 images with 600 images per class. We divide 100 into validation set per class and 250 into each subset group denoted as S_A and S_P. Ideally, we should not take advantage of labels from S_A at all cost. However, due to the forementioned challenge in autoencoder similarity search, we use S_A's labels to generate matching pairs by randomly sample 1000 pairs of images for each class, which results in a total number of 100,000 matching pairs.

CIFAR-100C [2] consists of CIFAR-100 dataset's images corrupted in 19 different contexts including Gaussian Blurring, snowing effects, and other background changes simulation in two severity level. We'll use *easy corruption* and *hard corruption* to indicate these two severity levels of corruption. The accuracy is calculated by averaging the accuracies in all 19 contexts of corruptions.

We use ResNet50 as the baseline model and backbone model for both Vanilla DRDJ and Adversarial DRDJ approaches. It is worth noted that the baseline is only trained on S_P which only consists of less than half of images from CIFAR-100 because we assume the labels are not accessible from S_A.

5.2 Metrics

Concluded from [13], accuracy doesn't imply robustness. One must evaluate the robustness of the model based on its relative performance (accuracy) to the baseline. We adopted a similar evaluation plot with regular test accuracy on the x-axis and corrupted test accuracy on the y-axis. An ideally perfect robust model should have accuracy aligned with the line $y = x$, which indicates no drop in corrupted accuracy compared to its regular test counterpart. We also plot the linear fit of all baseline models, which in our case is a series of ResNet50 in different configurations. A robust model should be positioned above the linear fit because it is expected to achieve better corrupted test accuracy than its similar-performance counterparts.

5.3 Vanilla DRDJ

Figure 2 shows constantly low performance of Vanilla DRDJ models. There is no obvious robustness in either easy or hard corruption. There are a number of potential failure reasons:

Relaxed Constraint Set. Previously, we use penalty term to avoid using Projected Gradient Descent that enforces the constraint set to hold. This might intrinsically break the theoretical guarantees and lead to a worse solution that becomes more and more pessimistic in prediction. During training, we observe that α_A and α_P usually don't follow the constraints they are meant to be within even with the penalty terms.

Weak Distribution Shift. In our experiments, we divide the same dataset CIFAR-100 into two groups. While there might exist some distribution shift in these two subsets, but they are minimal. The fact that $\tilde{P}_{S_A}$ and $\tilde{P}_{S_P}$ are much closer might sacrifice the accuracy for unrealistic robustness in some random worst case distribution.

Adaptation. Previously, we change the norm term and other terms in the objective to adjust to Multi-class image classification setting with neural networks. However, these simplifications are not supported by theoretical guarantees and might require more investigation than simply changing it to a desirable form at no cost.

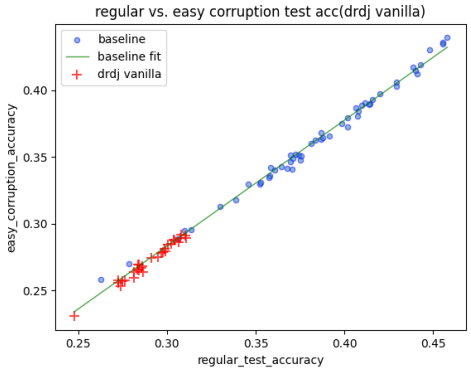

(a) Vanilla DRDJ on Easy Corruption

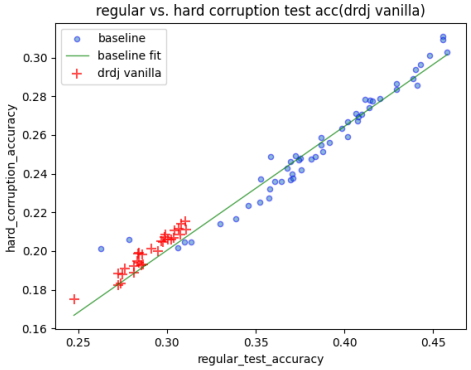

(b) Vanilla DRDJ on Hard Corruption

Figure 2: Vanilla DRDJ Evaluation on CIFAR-100C

5.4 Adversarial DRDJ

Figure 3 shows that under easy corruption, AT doesn't lead to a consistently robust model compared to the baseline. However, with harder corruption, we can see all the Adversarial DRDJ trained models have higher robustness because they are all positioned above the linear fit of the baseline. We also see that there is no overall lower trend in performance (regular test accuracy). This tells us that the AT DRDJ training approach is more tractable and easier to make the model learn the right solution.

Weak Distribution Shift. While the intuition set up previously is favorable, the simplifications done to split a dataset into two doesn't provide much meaningful distributions shift for our adversarial attack to be meaningful. The variance in adversarial attack will likely to override its intended effects when the corruption is not severe.

6 Future Direction

6.1 Revert Simplifications

Generating matching pairs with kNN. The matching pairs generation is simplified in this work due to time-constraints. Image data similarity search is primitively more difficult and time-consuming because of its high dimensional features. We aim to revisit autoencoder approach but also think of other alternatives since the pipeline involving training an antoencoder could be less tractable.

Incorporate auxiliary features. In this work, we didn't utilize any auxiliary features. We specify future directions for auxiliary features in Section 6.2.

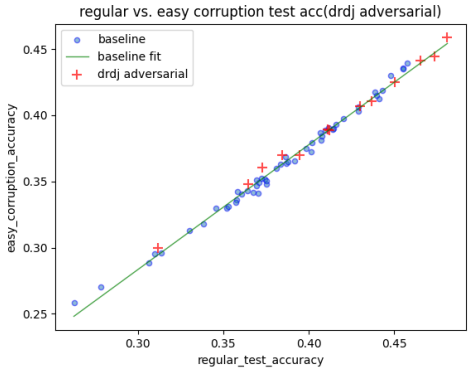

(a) Adversarial DRDJ on Easy Corruption

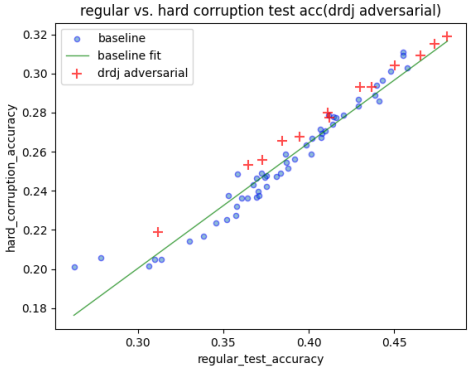

(b) Adversarial DRDJ on Hard Corruption

Figure 3: Adversarial DRDJ Evaluation on CIFAR-100C

Utilize unlabeled data from a natively different dataset. In our experiments, we split CIFAR-100 to two subsets and ignore the second subset's labels. However, such practice is not reflective of the target scenario this work is aiming at. Therefore, simulating the scenario with a dataset that (1) shares some features with the labeled set, (2) is unlabeled, and (3) provides larger amount of data, will be the ideal candidate for our next batch of experiments.

6.2 Auxiliary Features

For simplicity, we didn't explore auxiliary features in this work even though the proposed training approach is natively adaptive to auxiliary features. Additional features like metadata have promising potentials as explored by [14]. In addition, multimodal classification task can also be integrated into our proposed framework with some modifications as large video dataset with audio modality provides a lot of richness but requires tremendous labeling efforts. We aim to continue investigating more empirical results for multimodal tasks including audiovisual, text-visual, and other tabular metadata information.

6.3 Fairness

While the model's robustness is critical and the goal of this work, we believe this work also has potential impact on group fairness. Group information can be treated as auxiliary features in our work. Although the dataset with group information is unlabeled, our work allows incorporating group information in training an image classification model in tasks like facial recognition and provides more fair predictor than one trained purely on unbalanced and biased dataset with labels.

References

[1] Pranjal Awasthi, Christopher Jung, and Jamie Morgenstern. Distributionally robust data join. *arXiv preprint arXiv:2202.05797*, 2022.

[2] Dan Hendrycks and Thomas Dietterich. Benchmarking neural network robustness to common corruptions and perturbations. *Proceedings of the International Conference on Learning Representations*, 2019.

[3] Huaxiu Yao, Caroline Choi, Bochuan Cao, Yoonho Lee, Pang Wei W Koh, and Chelsea Finn. Wild-time: A benchmark of in-the-wild distribution shift over time. *Advances in Neural Information Processing Systems*, 35:10309–10324, 2022.

[4] Andrey Malinin, Neil Band, German Chesnokov, Yarin Gal, Mark JF Gales, Alexey Noskov, Andrey Ploskonosov, Liudmila Prokhorenkova, Ivan Provilkov, Vatsal Raina, et al. Shifts: A dataset of real distributional shift across multiple large-scale tasks. *arXiv preprint arXiv:2107.07455*, 2021.

[5] Hamed Rahimian and Sanjay Mehrotra. Distributionally robust optimization: A review. *arXiv preprint arXiv:1908.05659*, 2019.

[6] Emre Erdogan and Garud Iyengar. Ambiguous chance constrained problems and robust optimization. *Mathematical Programming*, 107:37–61, 2006. URL `https://api.semanticscholar.org/CorpusID:17811244`.

[7] Peyman Mohajerin Esfahani and Daniel Kuhn. Data-driven distributionally robust optimization using the wasserstein metric: Performance guarantees and tractable reformulations. *arXiv preprint arXiv:1505.05116*, 2015.

[8] Shiori Sagawa, Pang Wei Koh, Tatsunori B Hashimoto, and Percy Liang. Distributionally robust neural networks for group shifts: On the importance of regularization for worst-case generalization. *arXiv preprint arXiv:1911.08731*, 2019.

[9] Charlie Frogner, Sebastian Claici, Edward Chien, and Justin Solomon. Incorporating unlabeled data into distributionally robust learning. *arXiv preprint arXiv:1912.07729*, 2019.

[10] Matthew Staib. Distributionally robust deep learning as a generalization of adversarial training. 2017. URL `https://api.semanticscholar.org/CorpusID:52063282`.

[11] Yair Carmon, Aditi Raghunathan, Ludwig Schmidt, John C Duchi, and Percy S Liang. Unlabeled data improves adversarial robustness. *Advances in neural information processing systems*, 32, 2019.

[12] Kaiming He, Xinlei Chen, Saining Xie, Yanghao Li, Piotr Dollár, and Ross Girshick. Masked autoencoders are scalable vision learners. In *Proceedings of the IEEE/CVF conference on computer vision and pattern recognition*, pages 16000–16009, 2022.

[13] Rohan Taori, Achal Dave, Vaishaal Shankar, Nicholas Carlini, Benjamin Recht, and Ludwig Schmidt. Measuring robustness to natural distribution shifts in image classification. *Advances in Neural Information Processing Systems*, 33:18583–18599, 2020.

[14] Julian McAuley and Jure Leskovec. Image labeling on a network: using social-network metadata for image classification. In *Computer Vision–ECCV 2012: 12th European Conference on Computer Vision, Florence, Italy, October 7-13, 2012, Proceedings, Part IV 12*, pages 828–841. Springer, 2012.